Published in final edited form as:
Respir Physiol Neurobiol. 2012 March 15; 180(0): 193–203. doi:10.1016/j.resp.2011.11.006.

Carotid body growth during chronic postnatal hyperoxia

Elizabeth F. Dmitrieff, **Samantha E. Piro**, **Thomas A. Broge Jr.**, **Kyle B. Dunmire**, and **Ryan W. Bavis***
Department of Biology, Bates College, Lewiston, ME 04240 USA

Abstract

Rats reared in hyperoxia have smaller carotid bodies as adults. To study the time course and mechanisms underlying these changes, rats were reared in 60% O_2 from birth and their carotid bodies were harvested at various postnatal ages (P0-P7, P14). The carotid bodies of hyperoxia-reared rats were smaller than those of age-matched controls beginning at P4. In contrast, 7 days of 60% O_2 had no effect on carotid body size in rats exposed to hyperoxia as adults. Bromodeoxyuridine (BrdU) and TdT-mediated dUTP nick end labeling (TUNEL) were used to assess cell proliferation and DNA fragmentation at P2, P4, and P6. Hyperoxia reduced the proportion of glomus cells undergoing cell division at P4; although a similar trend was evident at P2, hyperoxia no longer affected cell proliferation by P6. The proportion of TUNEL-positive glomus cells was modestly increased by hyperoxia. We did not detect changes in mRNA expression for proapoptotic (Bax) or antiapoptotic (Bcl-X_L) genes or transcription factors that regulate cell cycle checkpoints (p53 or p21), although mRNA levels for cyclin B1 and cyclin B2 were reduced. Collectively, these data indicate that hyperoxia primarily attenuates postnatal growth of the carotid body by inhibiting glomus cell proliferation during the first few days of exposure.

Keywords

glomus cell; cell proliferation; developmental plasticity; control of breathing; gene expression

1. Introduction

The carotid body is the primary O_2 sensor in the mammalian respiratory control system and initiates protective ventilatory and arousal responses to acute hypoxia. This highly vascular organ is composed of several cell types, including glomus (type I) cells, sustentacular (type II) cells, nerve fibers, and endothelial cells; as much as 50–60% of the carotid body volume may be comprised of connective tissue (Wang & Bisgard, 2002). Although the mechanism of hypoxia transduction within the carotid body is not completely understood, it appears to be initiated in the glomus cell, a neuron-like secretory cell apposed to the terminals of carotid sinus nerve (CSN) axons. Hypoxia depolarizes the glomus cell, increases intracellular calcium, and triggers the release of neurochemicals, ultimately enhancing afferent nerve activity (Kumar, 2007; López-Barneo et al., 2008). Sustentacular cells, which

*Corresponding author: Ryan W. Bavis, PhD, Department of Biology, Bates College, 44 Campus Ave., Carnegie Science Hall, Lewiston, ME 04240 USA, Phone: 207-786-8269, Fax: 207-786-8334, rbavis@bates.edu.

envelop clusters of glomus cells, may serve glia-like functions in support of glomus cells and/or differentiate into glomus cells (Pardal et al., 2007).

The carotid body exhibits substantial morphological plasticity in response to chronic (i.e., days to weeks) changes in arterial O_2 tension. For example, chronic exposure to hypoxia causes the carotid body to increase in size in humans and other mammals, perhaps by as much as 2–4× depending on the duration of the stimulus (Wang & Bisgard, 2002; Kusakabe et al., 2003). In adult rats, carotid body size begins to increase within the first few days of hypoxia, plateaus by the fourth week of exposure, and returns to normal within a week after return to normoxia (Kusakabe et al., 2003, 2004; Wang et al., 2008). The increase in carotid body size is partly explained by vasodilation and vascular remodeling (Wang & Bisgard, 2002, 2005; Kusakabe et al., 2003; Wang et al., 2008). However, studies utilizing bromodeoxyuridine (BrdU) demonstrated large increases in the numbers of dividing glomus cells in neonatal (Wang & Bisgard, 2005) and adult (Wang et al., 2008) rats after 7 d in 12% O_2, indicating that glomus cell hyperplasia also contributes to carotid body enlargement; these researchers also observed hypoxia-induced proliferation of sustentacular and connective tissue cells, although the number of labeled cells tend to be smaller for these cell types. The increased numbers of glomus cells also may involve the proliferation and subsequent differentiation of sustentacular cells into glomus cells (Pardal et al., 2007).

In contrast to chronic hypoxia, chronic hyperoxia decreases carotid body size in neonatal rats (Erickson et al., 1998; Wang & Bisgard, 2005; Bavis et al., 2011a) and mice (Bavis et al., 2011a). Although the impact of chronic hyperoxia on carotid body size has not been reported for animals exposed *as adults*, chronic postnatal exposure to 60% O_2 (1–4 weeks) decreases carotid body size by approximately 40–75% (Erickson et al., 1998; Bisgard et al., 2003; Bavis et al., 2011a), with proportionate decreases in the volume occupied by glomus cells and non-glomic tissue (Erickson et al., 1998). The time course for the decrease in carotid body size has not previously been studied but, once decreased, this effect persists for months after the animal is returned to normoxia and appears to be permanent (Fuller et al., 2002).

The cellular and molecular mechanisms by which chronic postnatal hyperoxia decreases carotid body size, and more specifically the numbers of O_2-sensing glomus cells, are largely unstudied. At the cellular level, reduced carotid body size could reflect increased cell death, decreased cell proliferation, or some combination of these factors. Wang and Bisgard (2005) assessed cell death (TdT-mediated dUTP nick end labeling (TUNEL)) and proliferation (BrdU labeling) of carotid body glomus cells in 7 d old rats reared in 60% O_2. These authors did not detect TUNEL-positive cells in either control or hyperoxia-reared rats, but they observed fewer BrdU-positive glomus cells in the latter group. Although these data suggest that chronic hyperoxia inhibits cell proliferation, the total number of glomus cells was also reduced; thus, the reduced number of labeled cells could reflect the smaller initial cell population (perhaps due to earlier cell death) rather than inhibition of cell division *per se*. Moreover, it is possible that changes in cell survival and/or proliferation are more pronounced during the first few days of hyperoxia, as appears to be the case in chronic hypoxia (e.g., Wang et al., 2008). The primary objective of the present study, therefore, was to determine the proximate mechanism by which chronic hyperoxia reduces the number of carotid body glomus cells in neonatal rats. To this end, we studied the time course for changes in carotid body size during postnatal hyperoxia and asked whether similar hyperoxic exposures alter carotid body size in adult rats. Based on these findings, we used TUNEL and BrdU assays to evaluate the effects of hyperoxia on cell death and proliferation over the first six postnatal days.

High O_2 concentrations can cause oxidative injury and kill cells (necrosis), but studies in lung epithelium and other lung tissues indicate that hyperoxia also directly or indirectly activates intracellular signaling pathways that initiate programmed cell death (apoptosis) or inhibit cell proliferation. For example, oxidative damage to DNA increases mRNA and protein levels of the tumor suppressor protein p53 in the hyperoxic lung (O'Reilly et al., 1998a; O'Reilly, 2001; Perkowski et al., 2003), and this transcription factor regulates the expression of numerous genes related to apoptosis, cell cycle arrest, and DNA repair (Brown et al., 2007; Polager & Ginsberg, 2009). Among the proapoptotic genes regulated by p53, Bax is upregulated in the hyperoxic lung (McGrath-Morrow & Stahl, 2001; O'Reilly et al. 2000; Perkowski et al., 2003). However, oxidative injury can also arrest the cell cycle in the G_1 and G_2 phases of interphase (i.e., prior to DNA replication and mitosis, respectively) (O'Reilly, 2001); activation of these "checkpoints" enables the cell to repair DNA damage prior to cell division. The cyclin-dependent kinase inhibitor p21 is a major regulator of the G_1 checkpoint (O'Reilly, 2001, 2005), and it may also regulate the G_2 checkpoint (Gillis et al., 2009) and expression of the antiapoptotic protein Bcl-X_L (Wu & O'Reilly, 2011). Importantly, expression of p21 mRNA and protein increase in the hyperoxic lung (McGrath, 1998; O'Reilly et al., 1998b), and this increase is mediated by transcriptional activation by p53 as well as through p53-independent pathways (O'Reilly et al., 2001; O'Reilly, 2005). Increased p53 expression may also initiate G_2 arrest by inhibiting the transcription of the gene for cyclin B1 (Innocente & Lee, 2005; Innocente et al., 1999). Thus, to begin to identify molecular mechanisms for hyperoxia-induced changes in carotid body size, we examined the carotid body mRNA expression for several genes linked to apoptosis (Bax, Bcl-X_L) and diminished cell proliferation (p53, p21, cyclin B1, cyclin B2) in the hyperoxic lung. Since changes in carotid body size and glomus cell proliferation were well established by 4 d of age (see "Results"), we predicted that changes in gene expression causally linked to this plasticity would already be evident at 3 d of age.

2. Methods

2.1 Experimental animals

Timed-pregnant Sprague-Dawley rats were obtained from Charles River Laboratories (Portage, MI, USA), and offspring were studied as neonates (0 – 14 d of age; P0 – P14) or as adults. For hyperoxic exposures ("Hyperoxia" groups), rats were placed into an environmental chamber maintained at 60% O_2 (CO_2 <0.4%) on the day prior to birth (postnatal exposures) or at 19–20 weeks of age (adult exposures); for carotid body volume and immunohistochemistry experiments (see below), litters were culled to 10 on the day of birth. Chambers were opened briefly (<5 min) to remove animals for carotid body collection and to clean cages as needed. Individual Hyperoxia pups were kept with their mothers until studied (P0-P7 or P14). Rats exposed to hyperoxia as adults were removed from the chamber after 7 d for tissue collection. Age-matched litters or adults ("Control" groups) were reared under similar conditions but maintained at 21% O_2. Rats were maintained on a 12:12 light cycle throughout the study and provided food and water *ad libitum*.

All experimental procedures were approved by the Institutional Animal Care and Use Committee at Bates College.

2.2 Carotid body volumes

Carotid body volumes were measured to assess the effects of hyperoxia on carotid body size. Carotid body volumes were determined for neonates at P1, P3, P4, P5, P7, and P14 (day of birth = P0); three pups were taken from each of two litters per treatment group per age (n = 6 per treatment group per age). Carotid body volumes were determined for adult, male rats at 20–21 weeks of age (n = 6 per treatment group from 3 litters). Neonates were killed via

intracardiac injection of Beuthanasia-D solution (0.05 ml/10 g; Schering-Plough Animal Health Corp., Union, NJ, USA). Adult rats were killed via CO_2 inhalation and transcardially perfused with ice cold 4% paraformaldehyde (PFA) in 0.1 M phosphate buffered saline at pH 7.4 (PBS). Carotid bifurcations were dissected out *en bloc* and post-fixed in ice-cold 4% PFA in PBS for 1 h followed by cryoprotection in 30% sucrose in PBS for 24 h at 4°C. Carotid bifurcations were then embedded in Tissue-Tek O.C.T. compound (Sakura Finetek, Torrance, CA, USA) on dry ice and stored at −80°C until sectioned (9 μm for neonates, 12 μm for adults) with a cryostatic microtome and mounted onto slides (Fisherbrand Superfrost Plus). Slides were processed for morphological analysis using hematoxylin staining (neonates) or hematoxylin and eosin staining (adults).

Serial sections containing the carotid body were imaged with a Nikon Eclipse E800 microscope and RT color SPOT camera connected to SPOT Basic imaging software (Diagnostic Instruments Inc., Sterling Heights, MI, USA). The carotid body area was then calculated for each section using Image J software (National Institutes of Health, Bethesda, MD, USA); the investigator was blinded to the treatment group and age. Carotid body volume was estimated from the area of the carotid body on each section, section thickness, and the total number of sections containing the carotid body: Σ[carotid body area in each section (μm^2) × section thickness (μm)].

2.3 Carotid body blood vessel size

To assess changes in the size of carotid body blood vessels immediately following birth, the distribution of blood vessel size (cross-sectional area) was determined for carotid bodies of neonatal rats at P0, P2, and P4. Two pups were taken from each of three litters at each age studied (n = 6 individuals per age). Pups were decapitated, and carotid bifurcations were dissected out, processed, and frozen in the same manner as for carotid body volume measurements (see above). Carotid bifurcations were sectioned (12 μm) with a cryostatic microtome onto slides, and slides were then processed for morphological analysis using hematoxylin and eosin staining.

The three largest sections from each carotid body were imaged with a Nikon Eclipse 80i microscope attached to a 2 megapixel camera and NIS Elements software. Blood vessel areas (lumens only, and only if they appeared to be from cross-sections) were measured for each of the three carotid body sections; the investigator was blinded to the age group for each individual. Data were compiled into relative frequency histograms (bin width = 10 μm^2), and bins for each of the three sections were then averaged to obtain one value per bin per individual.

2.4 Immunohistochemistry for TUNEL, BrdU, and p21

Immunohistochemistry was used to assess BrdU, TUNEL, and p21 expression in the carotid bodies of neonatal Control and Hyperoxia rats. For TUNEL and BrdU labeling, pups were sampled from a total of 12 litters (n = 6 individuals taken from 2 litters per treatment group for each age studied). Rat pups for BrdU labeling were administered two intraperitoneal injections of BrdU (50 mg/kg in sterile saline; Sigma, St. Louis, MO, USA) 12 h apart on P1, P3, or P5 and killed via decapitation 24 h after the first injection (i.e., at P2, P4, and P6). Pups for TUNEL labeling were killed via decapitation at P2, P4, and P6. For p21, P3 rat pups were sampled from a total of 4 litters (n = 6 individuals taken from 2 litters per treatment group). Carotid bifurcations were dissected out, processed, frozen, and sectioned in the same manner as for carotid body volume (see above). The slides were stored at −80°C until immunohistochemical analysis.

For the TUNEL assay, three sections from the middle of each carotid body were labeled for tyrosine hydroxylase (TH; a marker for carotid body glomus cells) and nuclear DNA fragmentation by terminal deoxynucleotidyl transferase-mediated nick end-labeling. After a brief rinse in PBS, slides were fixed in 4% PFA for 15 min. Sections were rinsed 3 × 5 min in PBS and blocked in 10% normal goat serum (Jackson ImmunoResearch, West Grove, PA, USA) for 1 h. Sections were again rinsed in PBS and incubated overnight at 4°C with a rabbit anti-TH antibody (sc-14007, 1:50; Santa Cruz Biotechnology, Santa Cruz, CA, USA). Following three washes in PBS, slides were incubated with a Texas Red-conjugated goat anti-rabbit antibody (sc-2780, 1:100; Santa Cruz Biotechnology) for 90 min. TUNEL staining was then performed using a fluorescein-linked FragEL DNA fragmentation detection kit (EMD Biosciences, Gibbstown, NJ, USA) according to the manufacturer's cryosection protocol; the protocol was confirmed using positive control slides provided by the manufacturer (data not shown). Briefly, slides were rinsed in Tris-buffered saline (TBS) for 15 min and permeabilized for 10 min in proteinase K. Sections were then stained with the TdT labeling reaction mixture for 90 min and coverslipped with Fluorescein-FragEL mounting medium (EMD Biosciences).

For BrdU labeling, three sections from the middle of each carotid body were used for double immunofluorescence staining of TH and BrdU. After a brief rinse in PBS, sections were incubated for 2 h with 50% formamide in 2× SSC (0.3 M sodium citrate buffer containing 0.3 M sodium chloride) preheated to 65°C to denature the DNA. Following two rinses with 2× SSC, sections were soaked for 30 min in 2 M HCl at 37°C and then neutralized in 0.1 M borate buffer (pH 8.5) for 10 min. Sections were rinsed 3 × 5 min in PBS and blocked for 1 h with 10% normal goat serum (Jackson ImmunoResearch). Sections were first incubated with a mouse anti-BrdU monoclonal antibody (sc-32323, 1:50; Santa Cruz Biotechnology) overnight at 4°C. Sections were then rinsed in PBS and incubated with a biotinylated goat anti-mouse IgG1 (sc-2072, 1:100, Santa Cruz Biotechnology) for 1 h followed by a 30 min incubation with Rhodamine Red-X-conjugated streptavidin (016-290-084, 1:500; Jackson ImmunoResearch). After three 15 min washes in PBS, sections were incubated with a rabbit anti-TH antibody (sc-14007, 1:50; Santa Cruz Biotechnology) overnight at 4°C. Sections were then rinsed in PBS and incubated with a FITC-conjugated goat anti-rabbit secondary antibody (sc-2012, 1:100, Santa Cruz Biotechnology) for 90 min. The slides were rinsed and coverslipped with Vectashield HardSet mounting medium (Vector Labs, Burlingame, CA, USA).

For p21 labeling, the largest section from each carotid body was used for double immunofluorescence staining of TH and p21. After a brief rinse in PBS, cell membranes were permeabilized in 0.2% Triton X-100 in PBS for 30 min. After rinsing in PBS + 0.05% Tween 20 (PBST), sections were then blocked with 10% BlokHen (Aves Labs, Tigard, OR, USA)/10% normal donkey serum (Jackson ImmunoResearch) in PBS for 1 h in humidified chamber. After a brief rinse in PBST, sections were incubated with a rabbit anti-p21 polyclonal antibody (NB600-1139, 1:300; Novus Biologicals, Littleton, CO USA) and a chicken anti-TH polyclonal antibody (TYH, 1:1000; Aves Labs) overnight at 4°C. Sections were then rinsed in PBST and incubated with a donkey anti-rabbit secondary antibody conjugated to rhodamine (sc-2095, 1:100; Santa Cruz Biotechnology) and a goat anti-chicken secondary antibody conjugated to fluorescein (F-1005, 1:500; Aves Labs) for 1 h. The slides were rinsed and coverslipped with Vectashield HardSet mounting medium (Vector Labs, Burlingame, CA, USA).

After labeling, slides were imaged using a Nikon Eclipse 80i microscope with a 2 megapixel camera and NIS Elements software. For each image, the total number of TH-positive cells (glomus cells), the number of TUNEL-, BrdU-, or p21-positive glomus cells (i.e., co-expressing TH), and the number of TUNEL-, BrdU-, or p21-positive non-glomus cells were

counted. For TUNEL and BrdU assays, counts for three sections from the same carotid body were averaged to produce one value per individual. Data are reported as the ratio of labeled glomus cells to total glomus cells and as the ratio of labeled glomus cells to labeled non-glomus cells.

2.5 Quantitative RT-PCR

Total RNA was isolated from neonatal rat carotid bodies to assess the effects of hyperoxia on mRNA expression for several genes of interest (p21, p53, Bax, Bcl-X_L, cyclin B1, cyclin B2). To accomplish this, tissue was collected and processed in two separate rounds of experiments (experiment 1: p21, p53, Bax, Bcl-X_L; experiment 2: cyclin B1, cyclin B2). Different methods of cDNA synthesis and qRT-PCR amplification were used in these two experiments, which resulted in procedural differences in how samples were processed between the two rounds (see below). This difference should not impact the conclusions of this study, however, since comparisons between Control and Hyperoxia groups for each gene of interest are restricted to samples collected in the same experiment.

Three-day old (P3) pups were decapitated, and carotid bodies were harvested and either placed in 350 μl RNA*later* (Ambion, Austin, TX, USA) and frozen at −20°C (p21, p53, Bax, Bcl-X_L) or flash frozen on dry ice and stored at −80°C (cyclin B1 and B2). Due to the small size of the neonatal carotid body, each sample consisted of carotid bodies pooled from one litter (14 – 26 carotid bodies per pool). Carotid bodies were collected from a total of 7 or 6 litters per treatment group in experiments 1 and 2, respectively (i.e., n = 6–7 independent samples per treatment).

In each experiment, pooled carotid bodies were homogenized (rotor-stator) for 20 sec in RLT lysis buffer (Qiagen, Valencia, CA, USA). RNA was extracted from the homogenates using an RNeasy Micro RNA Isolation Kit (Qiagen) according to the manufacturer's protocol with the exception of doubling the DNase volume and incubation time for experiment 2 (cyclin B1 and cyclin B2); these modifications were recommended by the manufacturer to eliminate potential genomic contamination. RNA quantity and quality were assessed using an RNA 6000 Nano Chip in a Bioanalyzer (Agilent, Santa Clara, CA, USA). Total RNA yield averaged 0.6 μg per sample (31 ng per carotid body).

For p21, p53, Bax and Bcl-X_L, cDNA was synthesized from 200 ng total RNA using 1 μl ImProm-II Reverse Transcriptase, 1 μl primer mix (200 ng/μl oligo dT's and 50 ng/μl random hexamers), 1 μl 10 mM dNTPs, 4 μl ImProm-II 5× First strand buffer, and 2 μl 25 mM $MgCl_2$ (Promega), and 1 μl RNAseOUT (Invitrogen); these reactions were incubated at 25°C for 5 min followed by 42°C for 60 min and 70°C for 15 min. For cyclin B1 and cyclin B2, cDNA was synthesized from 300 ng total RNA using RT^2 First Strand Kit (SABiosciences, Frederick, MD USA) according to kit instructions with the exception of replacing GE Buffer with water. The resulting single-stranded cDNA products were either aliquoted undiluted (p21, p53, Bax and Bcl-X_L) or diluted with 36 μl RNase-free water prior to being aliquoted (cyclin B1 and cyclin B2). All cDNA samples were stored at −20°C until quantitative PCR analysis.

For the first experiment (p21, p53, Bax and Bcl-X_L), 2 genes of interest were assayed per 96-well plate. The reference gene β-actin was assayed on a separate 96-well plate and used to correct mRNA expression levels for differences in RNA quality and RT efficiency between samples (preliminary analysis indicated that β-actin was the most stable reference gene compared to TH, synaptophysin, chromogranin A, and β-III tubulin (geNORM v. 3.5, Ghent University Hospital Center for Medical Genetics, Belgium; data not shown)). Individual Control and Hyperoxia cDNA samples were run in triplicate (0.67 μl per well) for each gene of interest assayed and for β-actin. Primers were designed using NetPrimer

(PRIMIER Biosoft International, Palo Alto, CA, USA), with the exception of β-actin for which sequences were kindly provided by Dr. Gordon Mitchell (University of Wisconsin). All primer pairs for the first experiment (Table 1) were synthesized by Integrated DNA Technologies (Coralville, IA, USA). Primer pairs were validated prior to use and standard curve reaction efficiencies were determined to be between 90–110% (data not shown). Amplification was performed using Brilliant SYBR Green QPCR Master Mix (25 μl total reaction volume) in an Mx3000 qPCR System (Stratagene, Cedar Creek, TX, USA) as follows: 95°C × 10 min, 40 cycles of 95°C × 30 sec, 60/65°C × 1 min, 72°C × 30 sec (see Table 1 for annealing temperatures for individual assays).

For the second experiment (cyclin B1 and cyclin B2), each gene of interest and the reference gene β-actin were assayed on a separate 96-well plate. Individual Control and Hyperoxia cDNA samples were run in triplicate (1 μl per well) for each corresponding gene of interest and for β-actin. Primer pairs for use in the second experiment were obtained from SABiosciences: β-actin (Actb, cat. #PPR06570B; expected amplicon length: 131 bp), cyclin B1 (Ccnb1, cat. #PPR06572F; expected amplicon length: 94 bp), cyclin B2 (Ccnb2, cat. # PPR59595A; expected amplicon length: 86 bp). Amplification was performed using RT^2 Fast SYBR Green/ROX qPCR Master Mix (SABiosciences) in an Mx3000 qPCR System (Stratagene, Cedar Creek, TX, USA) as follows: 95°C × 10 min, 40 cycles of 95°C × 10 sec, 60°C × 30 sec.

Dissociation curve analyses were run for all assays in both experiments to confirm a single gene product in each well, and “no template” and “no reverse transcriptase” controls were included to monitor for genomic DNA and other contamination. All genes of interest were analyzed as follows: For each cDNA sample, triplicate C_T values were averaged to produce one value for the gene of interest and for β-actin. C_T values for the gene of interest were then normalized to β-actin C_T values using the $2^{-\Delta\Delta C_T}$ method (Livak and Schmittgen, 2001). Averaged $2^{-\Delta\Delta C_T}$values from the Control samples were used as the calibrator for the genes of interest, and mRNA expression is reported relative to the Control value (i.e., percent of Control).

2.6 Statistical analysis

To determine changes in body mass, carotid body volume, and proportions of TUNEL-, BrdU-, and p21-positive cells across multiple ages, Control and Hyperoxia treatment groups were compared by two-way analysis of variance (ANOVA) (factors: treatment, age) and Tukey’s *post hoc* tests. In some cases (i.e., carotid body volume), it was necessary to apply a logarithmic transformation prior to running the ANOVA to meet the equal variance assumption. The number of BrdU-positive glomus cells was also compared between Control and Hyperoxia groups separately at each age using analysis of covariance (ANCOVA), with the total number of glomus cells serving as a covariate. For adult rats, carotid body volume was compared between Control and Hyperoxia groups by independent samples t-tests. Median blood vessel size in Control carotid bodies was compared among age groups by a Kruskal-Wallis one-way ANOVA on ranks and Dunn’s *post hoc tests*. Carotid body mRNA expression for the genes of interest was compared between Control and Hyperoxia groups by Mann-Whitney U tests. Values are reported as mean±SEM, except as noted. Statistical tests were run using SigmaStat 3.1 or Systat 10.2 (ANCOVA) software.

3. Results

3.1 Effects of hyperoxia on carotid body volume in neonatal rats

The carotid body volume was determined at P1, P3, P4, P5, P7, and P14 for rats reared in 21% O_2 (Control) or 60% O_2 (Hyperoxia) (Fig. 1). There was a significant interaction

between treatment group and age for carotid body volume (treatment × age, P=0.001; Fig. 1A). In both treatment groups, the absolute size of the carotid body initially decreased, with the carotid body being ~50% smaller at P4 than at P1 (−43% and −56% in Control and Hyperoxia, respectively; both P<0.05). Although carotid body volume was similar between Control and Hyperoxia at P1 and P3, Hyperoxia carotid bodies were significantly smaller at P4 (P=0.03). Carotid bodies more than doubled in size between P4 and P14 in Control rats (+143%; P<0.001), but carotid bodies in Hyperoxia rats exhibited no growth over this period (P>0.05). Consequently, the size disparity between Control and Hyperoxia carotid bodies increased with age through P14 (Fig. 1A); at P14, the carotid bodies of Hyperoxia rats were only one-third the size of those in age-matched Controls (P<0.001).

Body mass increased dramatically between P1 and P14 as expected, but we also detected an interaction between treatment group and age (treatment × age, P<0.01); *post hoc* analysis revealed that Hyperoxia rats were significantly smaller than Control rats at P14 only (31.4±0.8 vs. 34.2±0.6 g). Although we previously have not observed an effect of chronic hyperoxia on body size (e.g., Bavis et al., 2010), we re-evaluated carotid body volumes after normalizing to body mass. Mass-specific carotid body volume decreased with age (Fig. 1B). As was the case for absolute carotid body volumes, there was a significant interaction between treatment group and age (treatment × age, P=0.002; Fig. 1B). Mass-specific carotid body volume tended to be lower in Hyperoxia rats at P4 (P=0.07), and this difference was statistically significant thereafter (i.e., P5, P7, and P14; all P≤0.001); no differences in carotid body volume were detected at P1 or P3. Thus, the analysis of absolute and mass-specific carotid body volumes yields similar results (i.e., diminished carotid body volume from approximately P4 through P14).

3.2 Effects of hyperoxia on carotid body volume in adult rats

To determine whether chronic hyperoxia influences carotid body size in adult rats, we exposed 19–20 week old rats to 60% O_2 for 7 d. Following this exposure, carotid body volume (Fig. 2A) and mass-specific carotid body volume (Fig. 2B) were not different between Control and Hyperoxia rats (P=0.37 and 0.23, respectively).

3.3 Effects of age on blood vessel size in Control rats

The initial decrease in carotid body volume observed in neonatal Control rats (P0–P4; Fig. 1A) was unexpected. The carotid body vasculature undergoes substantial remodeling following chronic hypoxia, as evidenced by a decrease in average blood vessel diameter (Kusakabe et al., 2004). Given the rise in arterial O_2 tension that accompanies the transition from a relatively hypoxic intrauterine environment, we investigated whether blood vessel size (gauged by lumen area) varies among P0, P2, and P4 rat carotid bodies. Small blood vessels (0–9.9 and 10.0–19.9 um^2) tended to be the most common at all ages (Fig. 3A–C). With increasing age, however, the proportion of blood vessels in the smallest size class (0–9.9 um^2) tended to increase. Accordingly, the median blood vessel lumen area varied with age (P=0.04; Fig. 3D); *post hoc* analysis revealed that the median blood vessel size was significantly smaller at P4 than at P0 (P<0.05).

3.4 Effects of hyperoxia on glomus cell DNA fragmentation and cell death

The TUNEL reaction detects DNA fragmentation and is often used to assess cell death by necrosis and apoptosis. TUNEL-positive cells were detected in the carotid body at all three ages studied (P2, P4, and P6), but the number of labeled cells was generally low (0 – 9 cells per carotid body section) (e.g., Fig. 4A). Labeling was observed in glomus cells (i.e., double-labeled for TUNEL and TH) as well as in other cell types (“non-glomus cells”). On average, less than 1% of all glomus cells were TUNEL-positive in a given section. However, the proportion of glomus cells that were TUNEL-positive was significantly greater in

Hyperoxia rats than in Control rats (0.7±0.1 vs. 0.3±0.1%, averaged across ages) (treatment, $P<0.01$; Fig. 4B); this ratio did not vary with age (age and treatment × age, both $P>0.05$).

To determine whether hyperoxia disproportionately affected glomus cells, we looked at the ratio of TUNEL-positive glomus cells to TUNEL-positive non-glomus cells. Approximately half of all TUNEL-positive cells were glomus cells (54±7%, averaged across all samples), and this ratio did not vary by age ($P=0.78$), treatment ($P=0.19$), or treatment × age ($P=0.79$). This suggests that hyperoxia increases DNA fragmentation and/or cell death in glomus and non-glomus cells at an equal rate.

3.5 Effects of hyperoxia on glomus cell proliferation

BrdU is stably incorporated into the DNA of dividing cells and is often used to assess cell proliferation. BrdU-positive cells were detected in the carotid body of Control and Hyperoxia rats at all three ages studied (P2, P4, and P6) (e.g., Fig. 5A). Our experimental protocol was expected to label cells undergoing DNA replication during the 24 h preceding tissue collection, indicating that carotid body cells were actively dividing P1–P2, P3–P4, and P5–P6 in both treatment groups. Labeling was observed in glomus cells (i.e., double-labeled for BrdU and TH) as well as in non-glomus cells.

The ratio of BrdU-positive glomus cells to the total number of glomus cells varied by age and treatment group (treatment × age, $P<0.01$; Fig. 5B). Specifically, the proportion of glomus cells that were BrdU-positive was significantly reduced at P2 ($P=0.04$) and P4 ($P<0.001$), but not at P6 ($P=0.28$). From P3 to P4, for example, our data suggest that approximately one-third as many glomus cells underwent cell division in Hyperoxia carotid bodies compared to age-matched Controls (i.e., 9±2 vs. 28±7% of glomus cells were BrdU-positive). Since overall carotid body volume was smaller at P4 and P6 in Hyperoxia rats (Fig. 1), we also compared the number of BrdU-positive glomus cells between treatment groups separately at each age by ANCOVA, with the total number of glomus cells serving as a covariate; this analysis reduces artifacts that may be introduced by changes in the denominator (total number of glomus cells) of the ratio (Packard & Boardman, 1999). ANCOVA confirmed that the number of BrdU-positive glomus cells was reduced in Hyperoxia rats at P4 ($P=0.001$) but not at P6 ($P=0.85$) (data not shown); although a trend toward reduced numbers of BrdU-positive glomus cells was also present at P2, the treatment effect did not reach statistical significance ($P=0.10$).

BrdU was detected in the nuclei of non-glomus cells as well (Fig. 5A). In Control rats, approximately half of all BrdU-positive cells were glomus cells. There was a trend for this proportion to be lower in Hyperoxia rats in all three age groups (Fig. 6), but this did not quite reach statistical significance (main effect for treatment, $P=0.06$); the ratio of BrdU-positive glomus cells to BrdU-positive non-glomus cells was not influenced by age (age and treatment × age, both $P>0.05$). These data suggest that chronic hyperoxia inhibits proliferation of both glomus cells and non-glomus cells.

3.6 Effects of hyperoxia on the expression of selected apoptosis and cell cycle genes

Carotid body mRNA expression was measured at P3 for several genes linked to the regulation of apoptosis (Bax, Bcl-X_L) and cell cycle progression (p53, p21, cyclin B1, cyclin B2). The relative expression of transcripts for Bax, Bcl-X_L, p53, and p21 did not differ between Control and Hyperoxia rats (all $P>0.05$) (Fig. 7A), although there was a trend toward a modest upregulation of Bcl-X_L in Hyperoxia ($P=0.06$). In contrast, we detected significant reductions in the mRNA expression for cyclin B1 (−60%; $P=0.04$)and cyclin B2 (−40%; $P<0.01$) in Hyperoxia carotid bodies (Fig. 7B). Cyclin B1 and cyclin B2 mRNA expression levels were assessed for carotid bodies collected from a different group of rats

than the other genes and using primer sets obtained from a commercial supplier. To confirm that these methodological differences did not influence our results, we re-analyzed mRNA expression for p21 using the same cDNA prepared for the cyclin B1 and cyclin B2 samples and using primers obtained from the same supplier (SABiosciences, cat# PPR06378A). The results of the second analysis were virtually identical to the first (i.e., no difference in p21 mRNA expression between Control and Hyperoxia carotid bodies) (data not shown).

To further confirm that p21 expression was not altered by chronic hyperoxia, we used immunohistochemistry to assess p21 protein in carotid body cells. Nuclear expression of p21 was observed in glomus cells (i.e., double-labeled for p21 and TH) as well as in non-glomus cells (Fig. 8), but very few cells exhibited obvious accumulation of p21 (0–17 cells per section). We did not attempt to quantify the relative expression of p21 in individual cells, but there was no evidence that chronic hyperoxia altered the proportion of glomus cells labeled for nuclear p21 (0.3±0.3 vs. 0.3±0.1% in Control and Hyperoxia, respectively; P=0.96).

4. Discussion

Rats and mice reared in chronic postnatal hyperoxia exhibit smaller carotid bodies (Erickson et al., 1998), and this effect persists for months despite returning to normoxia (Fuller et al., 2002; Bisgard et al., 2003; Bavis et al., 2011a). In the present study, we found that changes to carotid body volume are evident in neonatal rats after only 4–5 d in 60% O_2. In contrast, a one-week exposure to 60% O_2 had no effect on carotid body volume in rats exposed to hyperoxia as adults; this differs from the response to chronic hypoxia in which adult rats exhibit enlarged carotid bodies and substantial hyperplasia (Wang & Bisgard, 2003; Kusakabe et al., 2003; Pardal et al., 2007; Wang et al., 2008). Thus, as previously established for the hypoxic ventilatory response (HVR) (Ling et al., 1996, Bavis et al., 2002), there appears to be a critical period during early postnatal development in which carotid body morphology is susceptible to chronic increases in O_2 tension. Hyperoxia-induced changes in carotid body volume were accompanied by a marked reduction in cell proliferation (glomus cells and non-glomus cells) and a relatively small increase in DNA fragmentation/cell death. This is generally consistent with the findings of Wang & Bisgard (2005) who similarly concluded that hyperoxia primarily alters carotid body size by reducing new carotid body growth. Unlike that earlier study, however, which only showed a decreased number of dividing carotid body cells at P7 (which could reflect a smaller initial cell population), the present study specifically demonstrated a reduction in the *proportion* of dividing glomus cells, indicating inhibition of cell division; importantly, this effect was only detected at the earliest ages studied, P2 and P4, and not at P6. In contrast to hyperoxic lung injury (O'Reilly, 2001, 2005), p21 signaling does not appear to be a major pathway by which hyperoxia inhibits carotid body growth; however, we cannot rule out a potential role for p53-mediated inhibition of cyclin B gene transcription in slowing cell proliferation.

4.1 Carotid body growth in normoxia and chronic hyperoxia

Although the carotid body is known to increase in size during postnatal development (Clarke et al., 1990, 1993), this, to our knowledge, is the first study to examine carotid body growth in the early postnatal period. In rats reared in normoxia, absolute carotid body volume exhibited a biphasic pattern: an initial decrease in volume that reached a nadir around P4, followed by a rapid increase in volume from $_P$4-$_P$14. The initial decrease in carotid body volume, which was also observed in rats reared in hyperoxia, was unexpected. TUNEL-positive cells were observed in the neonatal carotid body at $_P$2, $_P$4, and $_P$6, so cell death may contribute to this decrease in size; no TUNEL-positive cells were evident at $_P$7 in an earlier study (Wang & Bisgard, 2005), suggesting apoptosis may be more common earlier in development. Given the relatively low frequency of TUNEL-positive cells, however, it is

unlikely that apoptosis alone could account for the >40% decrease in carotid body volume observed during this initial phase. Interestingly, normoxia-reared rats exhibited a decrease in average blood vessel size between P0 and P4 (i.e., 36% decrease in median lumen area). We propose that the decrease in blood vessel size, and thus part of the decrease in carotid body volume, reflects constriction and remodeling of blood vessels following the rise in arterial O_2 partial pressure (PO_2) at birth. Specifically, the transition from the relatively hypoxic *in utero* environment may be similar to the transition adult animals undergo following a chronic hypoxic exposure (i.e., rapid reversal of hypoxia-induced enlargement of blood vessels; Kusakabe et al., 2004). If increased blood vessel sizes equate to greater blood flow *in vivo*, these changes in carotid body vasculature may also alter carotid body PO_2 and influence the re-setting of carotid body O_2 sensitivity in the postnatal period (Carroll & Kim, 2005).

Carotid body volume was reduced after 4–5 d in 60% O_2, and the relative reduction in carotid body size may involve increased cell death and decreased proliferation of glomus cells and non-glomus cells (see below); although absolute volume was significantly lower at P4, the effect of hyperoxia on mass-specific volume was only marginally significant at P4 (P=0.06) and statistically significant thereafter. Chronic postnatal hyperoxia also prevented the secondary increase in carotid body volume between P4 and P14. Since BrdU-positive cells were observed in the carotid bodies of hyperoxia-reared rats during this time frame, this could indicate that the proliferation of new cells was offset by the death of existing cells and/or by changes in the volume of the vascular or extracellular compartments; the latter scenario appears unlikely, however, since the total volumes of glomic and non-glomic tissues diminish in parallel (Erickson et al., 1998). Alternatively, the number of new cells may not increase total organ volume sufficiently to be detected using our histological approach. The total number of glomus cells (and presumably non-glomus cells) is reduced after hyperoxia exposure (Wang & Bisgard, 2005; this study), so the number of new cells (and thus absolute growth rate) will be lower in hyperoxia even if the same proportion of cells divide in control and hyperoxia-reared rats; actually, the proportion of cells undergoing division was lower in hyperoxia-reared rats prior to P6. Even if the carotid body continues growing after the hyperoxic exposure is terminated (i.e., beyond P14), the carotid bodies of hyperoxia-reared animals remain considerably smaller than in age-matched controls throughout life (Fuller et al., 2002; Bisgard et al., 2003; Bavis et al., 2011a).

4.2 Hyperoxia-induced carotid body injury and/or cell death

High O_2 levels favor the production of reactive oxygen species (ROS) in excess of antioxidant defenses, potentially causing oxidative injury, necrosis, and/or apoptosis. Severe normobaric hyperoxia (>98% for 60–65 h) induces cellular damage and necrosis in glomus and sustentacular cells in neonatal and adult rats (DiGiulio et al., 1998), and the carotid body may be more susceptible to hyperoxic injury than other systemic tissues due to higher mass-specific blood flow (Mokashi & Lahiri, 1991). We observed a small, but statistically significant, increase in TUNEL-positive cells in 60% O_2 at P2, P4, and P6. The TUNEL assay detects DNA breaks, and positive labeling is usually interpreted as indicating cells in the late stages of apoptosis or necrosis. The small number of labeled carotid body cells in our study (e.g., <1% of glomus cells), however, suggests a relatively small contribution to the overall change in carotid body size. In contrast, 60% of parenchymal cells may be TUNEL-positive in the hyperoxic lung (O'Reilly, 2001); the greater rate of TUNEL-positive cells in the lung likely reflects both the higher inspired O_2 typically used to study hyperoxic lung injury (85–100% O_2) as well as the overall higher PO_2 in airways versus arterial blood.

Based on apparent discrepancies in the timing for first appearance of TUNEL-positive cells and other markers for apoptosis/necrosis in lung injury models, it has been suggested that the TUNEL assay also detects cells suffering DNA damage that ultimately will be repaired (O'Reilly, 2001). In other words, it is possible that some TUNEL-positive cells will not die

and, consequently, will not impact carotid body size. This may help to explain why we did not detect changes in carotid body mRNA expression for Bax (proapoptotic) and Bcl-X_L (antiapoptotic) in hyperoxia-reared rats despite the observed increase in TUNEL-positive cells. This may also explain why chronic hyperoxia did not decrease carotid body size in rats exposed as adults, as might have been expected if arterial P_{O_2} during 60% O_2 is sufficient to induce cell death.

4.3 Inhibition of carotid body cell proliferation

The proportion of glomus cells that had undergone cell division in the previous 24 h was markedly reduced by chronic hyperoxia at P4; although the absolute number of BrdU-positive cells was reduced at P6 (data not shown; see also Wang & Bisgard, 2005), the ratio of BrdU-positive glomus cells to total glomus cells was not significantly different at this age. Although hyperoxia tended to reduce glomus cell proliferation at P2 as well, the statistical analysis for this age group was equivocal: the proportion of glomus cells that were BrdU-positive was significantly reduced (Fig. 5B), but this effect was not significant using an alternate statistical test (ANCOVA) despite detecting a similar trend. These data indicate that chronic hyperoxia inhibits the normal proliferation of glomus cells during the early postnatal growth of the carotid body. We did not use cell-specific markers for other cell types, so we did not quantify the effect of hyperoxia on proliferation of non-glomus cells; however, given that the ratio of BrdU-positive glomus cells to BrdU-positive non-glomus cells was unchanged in hyperoxia-reared rats (Fig. 6), it appears that hyperoxia inhibits the proliferation of multiple cell types within the carotid body.

The mechanism(s) by which hyperoxia inhibits carotid body cell proliferation remains unclear. We hypothesized that hyperoxia would activate p53 and p21 signaling pathways, perhaps through DNA damage, ultimately arresting the cell cycle. It is not surprising that p53 mRNA expression did not change. Although p53 transcription may increase in the hyperoxic lung (Perkowski et al., 2003), p53 signaling is primarily regulated at the protein level (O'Reilly et al., 1998a; O'Reilly, 2001; Brown et al., 2007). However, chronic hyperoxia also did not increase mRNA expression for p21, a major regulator of the G_1 checkpoint that is transcriptionally regulated by p53, nor was there an obvious increase in p21 protein accumulation in carotid body cells. Thus, there currently is no evidence that hyperoxia slows carotid body growth through a p21-dependent pathway. On the other hand, cyclin B1 and cyclin B2 mRNA expression levels were reduced in hyperoxia-reared rats. Cyclin B proteins are essential for progression from G_2 into mitosis, so low cyclin B transcript levels may indicate activation of a G_2 checkpoint. This could be mediated by p53, which represses transcription of cyclin B1 (Innocente & Lee, 2005; Innocente et al., 1999; cyclin B2 was not studied), although it seems likely that p21 transcription would have been upregulated as well if p53 were activated. It is possible that decreased cyclin B1 and cyclin B2 mRNA expression is an artifact of fewer carotid body cells undergoing mitosis; however, in a preliminary study (n=2 Control and 2 Hyperoxia), we detected significant downregulation of cyclin B1 and cyclin B2 mRNA in hyperoxia, but no change in transcript levels for other proteins that vary expression across the cell cycle (e.g., cyclin A2 and proliferating cell nuclear antigen) (E.F. Dmitrieff & R.W. Bavis, unpublished observations).

Although p53 and p21 are key regulators of cell cycle checkpoints in hyperoxic lung injury, it is known that DNA damage can activate checkpoints through many distinct molecular pathways (O'Reilly, 2001); the potential contributions of these pathways to hyperoxia-induced changes in carotid body morphology await study. Alternatively, it is possible that hyperoxia influences the expression and/or activity of mitogens (i.e., reducing the stimulus for cell division) rather than activating checkpoints through oxidative injury. For example, carotid body glomus and sustentacular cells express numerous growth factors that stimulate cell proliferation and enhance cell survival (Wang & Bisgard, 2005; Izal-Azcárate et al.,

2008; Porzionato et al., 2008), and protein levels for at least one of these, brain-derived neurotrophic factor (BDNF), is reduced in the carotid bodies of hyperoxia-reared rats (Dmitrieff et al., 2011). The role of BDNF in proliferation of glomus cells has not been studied; however, glomus cells express TrkB receptors (Wang & Bisgard, 2005; Dmitrieff et al., 2011), consistent with an autocrine role for BDNF in carotid body growth and development. If oxidative damage is not a prerequisite for growth inhibition, this could explain why antioxidant treatments do not prevent changes to carotid body size during chronic exposure to 60% O_2 (Bavis et al., 2008).

4.4 Functional implications of reduced carotid body size

Given their primary role in O_2 transduction, reduced numbers of glomus cells likely contribute to the diminished HVR observed after chronic postnatal hyperoxia (Hanson et al., 1989; Ling et al., 1996; Bavis et al., 2010, 2011). Moreover, glomus cells are the primary source of BDNF and glial cell-line derived neurotophic factor (GDNF) in the carotid body (Wang & Bisgard, 2005; Izal-Azcárate et al., 2008), and these neurotrophins are required for the survival of sensory neurons that innervate the carotid body (Brady et al., 1999; Erickson et al., 2001); thus, loss of glomus cells likely contributes the degeneration of chemoafferent neurons observed during postnatal hyperoxia (Erickson et al., 1998). The O_2 sensitivity of individual chemoreceptor cells is also reduced after 4–5 d in 60% O_2 (Donnelly et al., 2008; Bavis et al., 2011b). While changes in carotid body size and chemoreceptor O_2 sensitivity are likely independent responses to chronic hyperoxia, the combined effect should be a substantial reduction in the whole-carotid body response to hypoxia by P4. Indeed, normoxic ventilation is reduced at P4 in rats reared in 60% O_2 from birth (Bavis et al., 2010), which could reflect diminished carotid body contribution to respiratory drive. Interestingly, despite being blunted at P7 and P14, the early, carotid body-mediated phase of the HVR is normal at P4 in hyperoxia-reared rats (Bavis et al., 2010). The disparity between the onset of carotid body impairment and blunting of the early HVR may indicate some degree of compensation in the central nervous system (CNS). The late HVR, which reflects a balance between carotid body stimulation and central inhibitory processes, is enhanced in P4 hyperoxia-reared rats (Bavis et al., 2010), consistent with excitatory plasticity in the CNS.

4.5 Significance

The present study confirms that hyperoxia, like hypoxia, has profound effects on carotid body morphology. Unlike hypoxia, however, which stimulates cell proliferation even in adult animals, hyperoxia only affects carotid body size in the immature carotid body. The capacity for brief exposures to moderate hyperoxia to inhibit normal postnatal carotid body growth may have important implications for preterm and very low birthweight infants that receive O_2 therapy. Despite widespread recognition of the importance of minimizing O_2 exposures, preterm infants are hyperoxic relative to target oxygenation levels for 30–40% of the time they are on supplemental O_2, and some individuals may be hyperoxic 90% of the time (Hagadorn et al., 2006; Finer & Leone, 2009; Claure & Bancalari, 2009). Moreover, it is known that preterm infants previously treated with supplemental O_2 may have abnormal peripheral chemoreceptor function (Calder et al., 1994; Katz-Salamon & Lagercrantz, 1994) and that this is related to the duration of the O_2 treatment (Katz-Salamon & Lagercrantz, 1994). Collectively, these observations raise important questions regarding the potential impact of supplemental O_2 on respiratory control development.

Highlights

We studied the effects of chronic hyperoxia on carotid body development in rats.
Hyperoxia reduced carotid body size within 4 days in neonatal rats, but not adults.

Reduced carotid body size was associated with decreased cell division. Hyperoxia modestly increased the proportion of TUNEL-positive glomus cells. Hyperoxia decreased mRNA for cyclins B1 and B2, but no change in other genes studied.

Acknowledgments

This study was supported by grant number P20 RR-016463 from the National Center for Research Resources (NCRR), a component of NIH. Its contents are solely the responsibility of the authors and do not necessarily represent the official views of NCRR or NIH.

References

Bavis RW, Olson EB Jr, Mitchell GS. Critical developmental period for hyperoxia-induced blunting of hypoxic phrenic responses in rats. J. Appl. Physiol. 2002; 92:1013–1018. [PubMed: 11842034]

Bavis RW, Wenninger JM, Miller BM, Dmitrieff EK, Olson EB Jr, Mitchell GS, Bisgard GE. Respiratory plasticity after perinatal hyperoxia is not prevented by antioxidant supplementation. Respir. Physiol. Neurobiol. 2008; 160:301–312.

Bavis RW, Young KM, Barry KJ, Boller MR, Kim E, Klein PM, Ovrutsky AR, Rampersad DA. Chronic hyperoxia alters the early and late phases of the hypoxic ventilatory response in neonatal rats. J. Appl. Physiol. 2010; 109:796–803. [PubMed: 20576840]

Bavis RW, Dmitrieff EF, Young KM, Piro SE. Hypoxic ventilatory response of adult rats and mice after developmental hyperoxia. Respir. Physiol. Neurobiol. 2011a; 177:342–346. [PubMed: 21601659]

Bavis RW, Kim I, Pradhan N, Nawreen N, Dmitrieff EF, Carroll JL, Donnelly DF. Recovery of carotid body O_2 sensitivity following chronic postnatal hyperoxia in rats. Respir. Physiol. Neurobiol. 2011b; 177:47–55. [PubMed: 21420511]

Bisgard GE, Olson EB Jr, Wang Z-Y, Bavis RW, Fuller DD, Mitchell GS. Adult carotid chemoafferent responses to hypoxia after 1, 2, and 4 wk of postnatal hyperoxia. J. Appl. Physiol. 2003; 95:946–952. [PubMed: 12909596]

Brady R, Zaidi SI, Mayer C, Katz DM. BDNF is a target-derived survival factor for arterial baroreceptor and chemoafferent primary sensory neurons. J. Neurosci. 1999; 19:2131–2142. [PubMed: 10066266]

Brown L, Boswell S, Raj L, Lee SW. Transcriptional targets of p53 that regulate cellular proliferation. Crit. Rev. Eukaryot. Gene Expr. 2007; 17:73–85. [PubMed: 17361486]

Calder NA, Williams BA, Smyth J, Boon AW, Kumar P, Hanson MA. Absence of ventilatory response to alternating breaths of mild hypoxia and air in infants who have had bronchopulmonary dysplasia: implications for the risk of sudden infant death. Pediatr. Res. 1994; 35:677–681. [PubMed: 7936817]

Carroll JL, Kim I. Postnatal development of carotid body glomus cell O_2 sensitivity. Respir. Physiol. Neurobiol. 2005; 149:201–215. [PubMed: 15886071]

Clarke JA, de Burgh Daly M, Ead HW. Comparison of the size of the vascular ompartment of the carotid body of the fetal, neonatal and adult cat. Acta Anat. (Basel). 1990; 138:166–174. [PubMed: 2368608]

Clarke JA, Daly MD, Ead HW. Vascular analysis of the carotid body in the spontaneously hypertensive rat. Adv. Exp. Med. Biol. 1993; 337:3–8. [PubMed: 8109413]

Claure N, Bancalari E. Automated respiratory support in newborn infants. Semin. Fetal Neonatal Med. 2009; 14:35–41. [PubMed: 18829405]

Di Giulio C, Di Muzio M, Sabatino G, Spoletini L, Amicarelli F, Di Ilio C, Modesti A. Effect of chronic hyperoxia on young and old rat carotid body ultrastructure. Exp. Gerontol. 1998; 33:319–329. [PubMed: 9639168]

Dmitrieff EF, Wilson JT, Dunmire KB, Bavis RW. Chronic hyperoxia alters the expression of neurotrophic factors in the carotid body of neonatal rats. Respir. Physiol. Neurobiol. 2011; 175:220–227. [PubMed: 21094282]

Donnelly DF, Bavis RW, Kim I, Dbouk HA, Carroll JL. Time course of alterations in pre- and post-synaptic chemoreceptor function during developmental hyperoxia. Respir. Physiol. Neurobiol. 2009; 168:189–197. [PubMed: 19465165]

Erickson JT, Mayer C, Jawa A, Ling L, Olson EB Jr, Vidruk EH, Mitchell GS, Katz DM. Chemoafferent degeneration and carotid body hypoplasia following chronic yperoxia in newborn rats. J. Physiol. 1998; 509:519–526. [PubMed: 9575300]

Erickson JT, Brosenitsch TA, Katz DM. Brain-derived neurotrophic factor and glial cell line-derived neurotrophic factor are required simultaneously for survival of dopaminergic primary sensory neurons *in vivo* . J. Neurosci. 2001; 21:581–589. [PubMed: 11160437]

Finer N, Leone T. Oxygen saturation monitoring for the preterm infant: the evidence basis for current practice. Pediatr. Res. 2009; 65:375–380. [PubMed: 19127213]

Fuller DD, Bavis RW, Vidruk EH, Wang Z-Y, Olson EB Jr, Bisgard GE, Mitchell GS. Life-long impairment of hypoxic phrenic responses in rats following 1 month of developmental hyperoxia. J. Physiol. 2002; 538:947–955. [PubMed: 11826178]

Gillis LD, Leidal AM, Hill R, Lee PW. $p21^{Cip1/WAF1}$ mediates cyclin B1 degradation in response to DNA damage. Cell Cycle. 2009; 8:253–256. [PubMed: 19158493]

Hagadorn JI, Furey AM, Nghiem TH, Schmid CH, Phelps DL, Pillers DA, Cole CH. AVIOx Study Group Achieved versus intended pulse oximeter saturation in infants born less than 28 weeks' gestation: the AVIOx study. Pediatrics. 2006; 118:1574–1582. [PubMed: 17015549]

Hanson, MA.; Eden, GJ.; Nijhuis, JG.; Moore, PJ. Peripheral chemoreceptors and other oxygen sensors in the fetus and newborn. In: Lahiri, S.; Forster, RE.; Davies, RO.; Pack, AI., editors. Chemoreceptors and Reflexes in Breathing: Cellular and Molecular Aspects. New York: Oxford University Press; 1989. p. 113-120.

Innocente SA, Lee JM. p53 is a NF-Y- and p21-independent, Sp1-dependent repressor of cyclin B1 transcription. FEBS Lett. 2005; 579:1001–1007. [PubMed: 15710382]

Innocente SA, Abrahamson JL, Cogswell JP, Lee JM. p53 regulates a G_2 checkpoint through cyclin B1. Proc. Natl. Acad. Sci. U.S.A. 1999; 96:2147–2152. [PubMed: 10051609]

Izal-Azcárate A, Belzunegui S, San Sebastián W, Garrido-Gil P, Vázquez-Claverie M, López B, Marcilla I, Luquin MA. Immunohistochemical characterization of the rat carotid body. Respir. Physiol. Neurobiol. 2008; 161:95–99. [PubMed: 18280799]

Katz-Salamon M, Lagercrantz H. Hypoxic ventilatory defense in very preterm infants: attenuation after long term oxygen treatment. Arch. Dis. Child Fetal Neonatal Ed. 1994; 70:F-90–F-95. [PubMed: 8154920]

Kumar P. Sensing hypoxia in the carotid body: from stimulus to response. Essays Biochem. 2007; 43:43–60. [PubMed: 17705792]

Kusakabe T, Hirakawa H, Matsuda H, Kawakami T, Takenaka T, Hayashida Y. Peptidergic innervation in the rat carotid body after 2, 4, and 8 weeks of hypocapnic hypoxic exposure. Histol. Histopathol. 2003; 18:409–418. [PubMed: 12647791]

Kusakabe T, Hirakawa H, Oikawa S, Matsuda H, Kawakami T, Takenaka T, Hayashida Y. Morphological changes in the rat carotid body 1, 2, 4, and 8 weeks after the termination of chronically hypocapnic hypoxia. Histol. Histopathol. 2004; 19:1133–1140. [PubMed: 15375756]

Ling L, Olson EB Jr, Vidruk EH, Mitchell GS. Attenuation of the hypoxic ventilatory response in adult rats following one month of perinatal hyperoxia. J. Physiol. 1996; 495:561–571. [PubMed: 8887766]

Livak KJ, Schmittgen TD. Analysis of relative gene expression data using real-time quantitative PCR and the $2^{-\Delta\Delta C}T$ method. Methods. 2001; 25:402–408. [PubMed: 11846609]

López-Barneo J, Ortega-Sáenz P, Pardal R, Pascual A, Piruat JI. Carotid body oxygen sensing. Eur. Respir. J. 2008; 32:1386–1398. [PubMed: 18978138]

McGrath SA. Induction of $p21^{WAF/CIP1}$ during hyperoxia. Am. J. Respir. Cell. Mol. Biol. 1998; 18:179–187. [PubMed: 9476904]

McGrath-Morrow SA, Stahl J. Apoptosis in neonatal murine lung exposed to hyperoxia. Am. J. Respir. Cell. Mol. Biol. 2001; 25:150–155. [PubMed: 11509323]

Mokashi A, Lahiri S. Aortic and carotid body chemoreception in prolonged hyperoxia in the cat. Respir. Physiol. 1991; 86:233–243. [PubMed: 1780602]

O'Reilly MA. DNA damage and cell cycle checkpoints in hyperoxic lung injury: braking to facilitate repair. Am. J. Physiol. Lung Cell. Mol. Physiol. 2001; 281:L291–L305. [PubMed: 11435201]

O'Reilly MA. Redox activation of $p21^{Cip1/WAF1/Sdi1}$: a multifunctional regulator of cell survival and death. Antioxid. Redox Signal. 2005; 7:108–118. [PubMed: 15650400]

O'Reilly MA, Staversky RJ, Stripp BR, Finkelstein JN. Exposure to hyperoxia induces p53 expression in mouse lung epithelium. Am. J. Respir. Cell. Mol. Biol. 1998a; 18:43–50. [PubMed: 9448044]

O'Reilly MA, Staversky RJ, Watkins RH, Maniscalco WM. Accumulation of $p21^{Cip1/WAF1}$ during hyperoxic lung injury in mice. Am. J. Respir. Cell. Mol. Biol. 1998b; 19:777–785. [PubMed: 9806742]

O'Reilly MA, Staversky RJ, Huyck HL, Watkins RH, LoMonaco MB, D'Angio CT, Baggs RB, Maniscalco WM, Pryhuber GS. Bcl-2 family gene expression during severe hyperoxia induced lung injury. Lab. Invest. 2000; 80:1845–1854. [PubMed: 11140697]

O'Reilly MA, Staversky RJ, Watkins RH, Reed CK, de Mesy Jensen KL, Finkelstein JN, Keng PC. The cyclin-dependent kinase inhibitor p21 protects the lung from oxidative stress. Am. J. RespirCell. Mol. Biol. 2001; 24:703–710.

Packard GC, Boardman TJ. The use of percentages and size-specific indices to normalize physiological data for variation in body size: wasted time, wasted effort? Comp. Biochem Physiol. 1999; A 122:37–44.

Pardal R, Ortega-Sáenz P, Durán R, López-Barneo J. Glia-like stem cells sustain physiologic neurogenesis in the adult mammalian carotid body. Cell. 2007; 131:364–377. [PubMed: 17956736]

Perkowski S, Sun J, Singhal S, Santiago J, Leikauf GD, Albelda SM. Gene expression profiling of the early pulmonary response to hyperoxia in mice. Am. J. Respir. Cell. Mol. Biol. 2003; 28:682–696. [PubMed: 12760966]

Polager S, Ginsberg D. p53 and E2f: partners in life and death. Nat. Rev. Cancer. 2009; 9:738–748. [PubMed: 19776743]

Porzionato A, Macchi V, Parenti A, De Caro R. Trophic factors in the carotid body. Int. Rev. Cell. Mol. Biol. 2008; 269:1–58. [PubMed: 18779056]

Wang Z-Y, Bisgard GE. Chronic hypoxia-induced morphological and neurochemical changes in the carotid body. Microsc. Res. Tech. 2002; 59:168–177. [PubMed: 12384961]

Wang Z-Y, Bisgard GE. Postnatal growth of the carotid body. Respir. Physiol. Neurobiol. 2005; 149:181–190. [PubMed: 15914098]

Wang Z-Y, Olson EB Jr, Bjorling DE, Mitchell GS, Bisgard GE. Sustained hypoxia-induced proliferation of carotid body type I cells in rats. J. Appl. Physiol. 2008; 104:803–808. [PubMed: 18096755]

Wu YC, O'Reilly MA. Bcl-X_L is the primary mediator of p21 protection against hyperoxia-induced cell death. Exp. Lung Res. 2011; 37:82–91. [PubMed: 21128858]

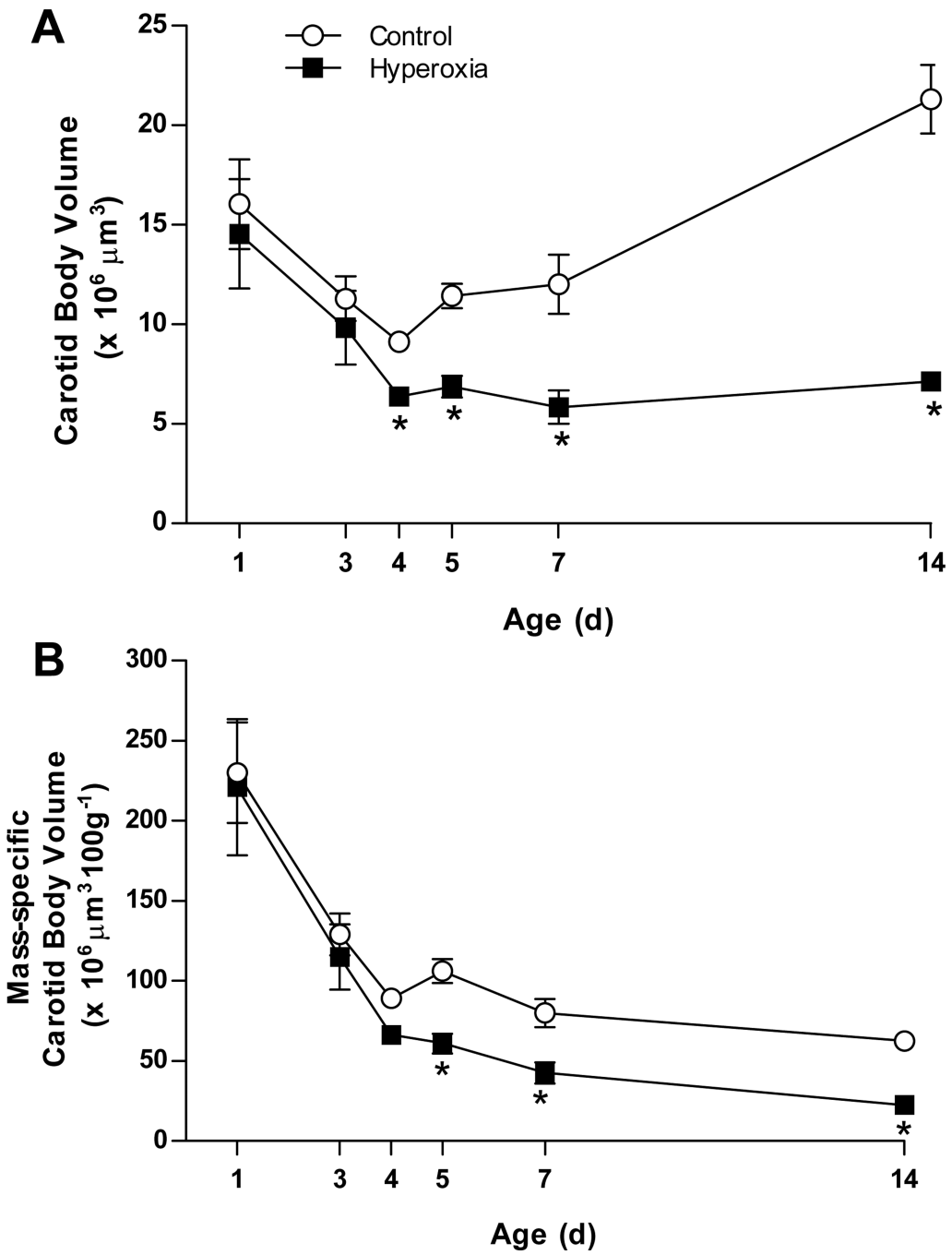

Fig. 1.

Carotid body growth in neonatal rats reared in 21% O_2 (Control) or 60% O_2 (Hyperoxia). Carotid body volumes are expressed (A) in absolute units and (B) normalized to body mass. Values are mean ± SEM; n= 6 per treatment group per age. * P<0.05 vs. Control at the same age.

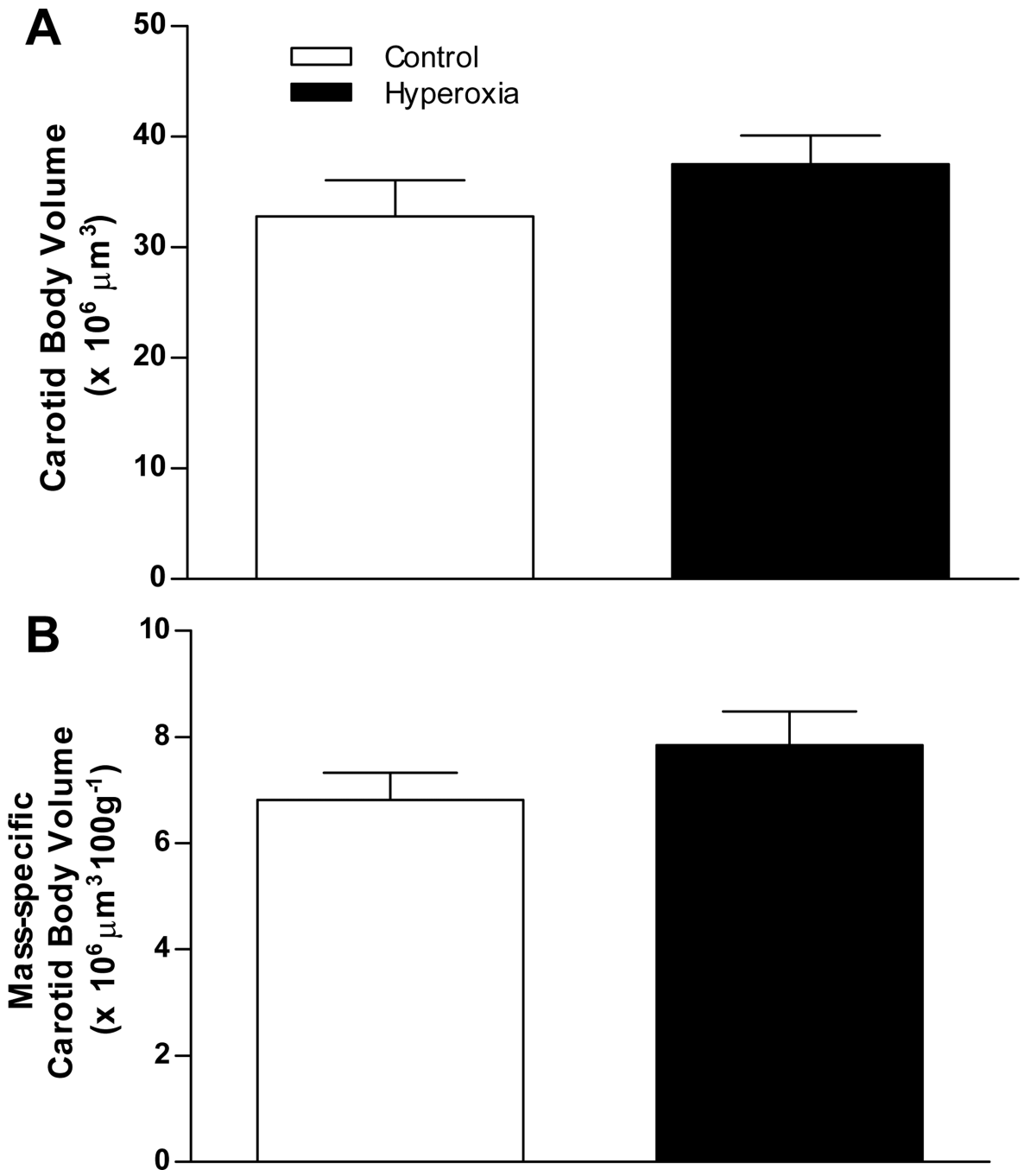

Fig. 2.

Carotid body size in adult rats (20–21 wks of age) exposed *as adults* to 7 d of 21% O_2 (Control) or 60% O_2 (Hyperoxia). Carotid body volumes are expressed (A) in absolute units and (B) normalized to body mass. Values are mean ± SEM; n= 6 per treatment group. No significant differences were detected between treatment groups.

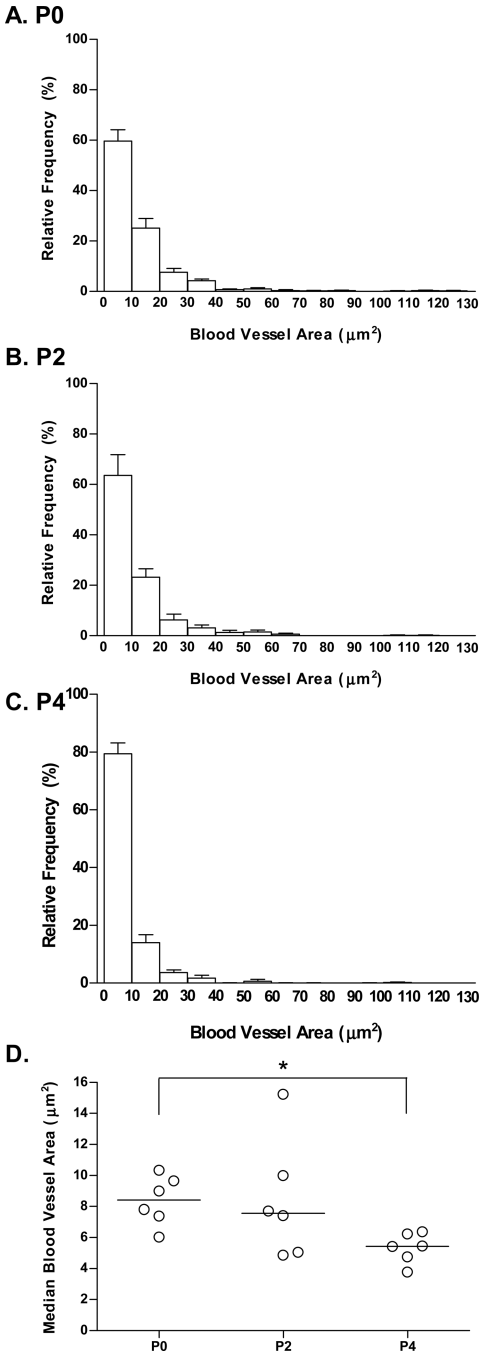

Fig. 3.

Distribution of carotid body blood vessel size (cross-sectional area of lumen) during the early postnatal period for rats reared in 21% O_2. Panels A–C depict relative frequency distributions for blood vessel areas at P0, P2, and P4, respectively. Values are mean ± SEM; n = 6 per treatment group. In Panel D, the median blood vessel size is plotted for each age group; each data point represents the median blood vessel size for one individual, and horizontal lines indicate the median for each group. * $P<0.05$ vs. P0.

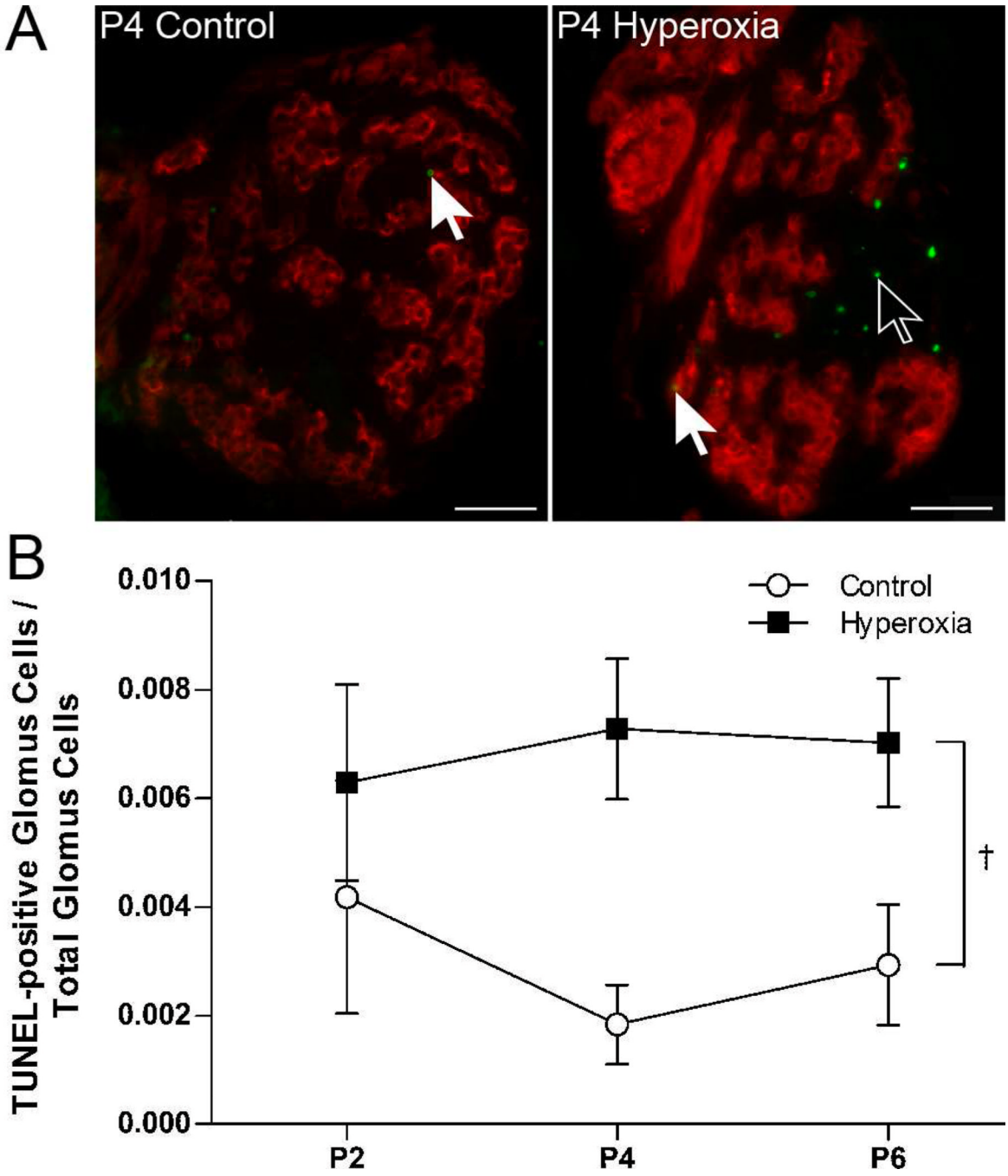

Fig. 4.

(A) Representative photomicrographs showing TUNEL-positive cells in the carotid bodies of P4 rats reared in 21% O_2 (Control) or 60% O_2 (Hyperoxia). Red fluorescence indicates staining for tyrosine hydroxylase, a marker for glomus cells, and green fluorescence indicates positive staining for DNA fragmentation (TUNEL). Closed arrows point to TUNEL-positive glomus cells (red and green); open arrows point to TUNEL-positive non-glomus cells (green only). Scale bar = 50 μm. (B) The ratio of TUNEL-positive glomus cells to the total number of glomus cells in Control and Hyperoxia rats at P2, P4, and P6. Values are mean ± SEM; n = 6 per treatment group per age. †Significant main effect for treatment (P<0.05).

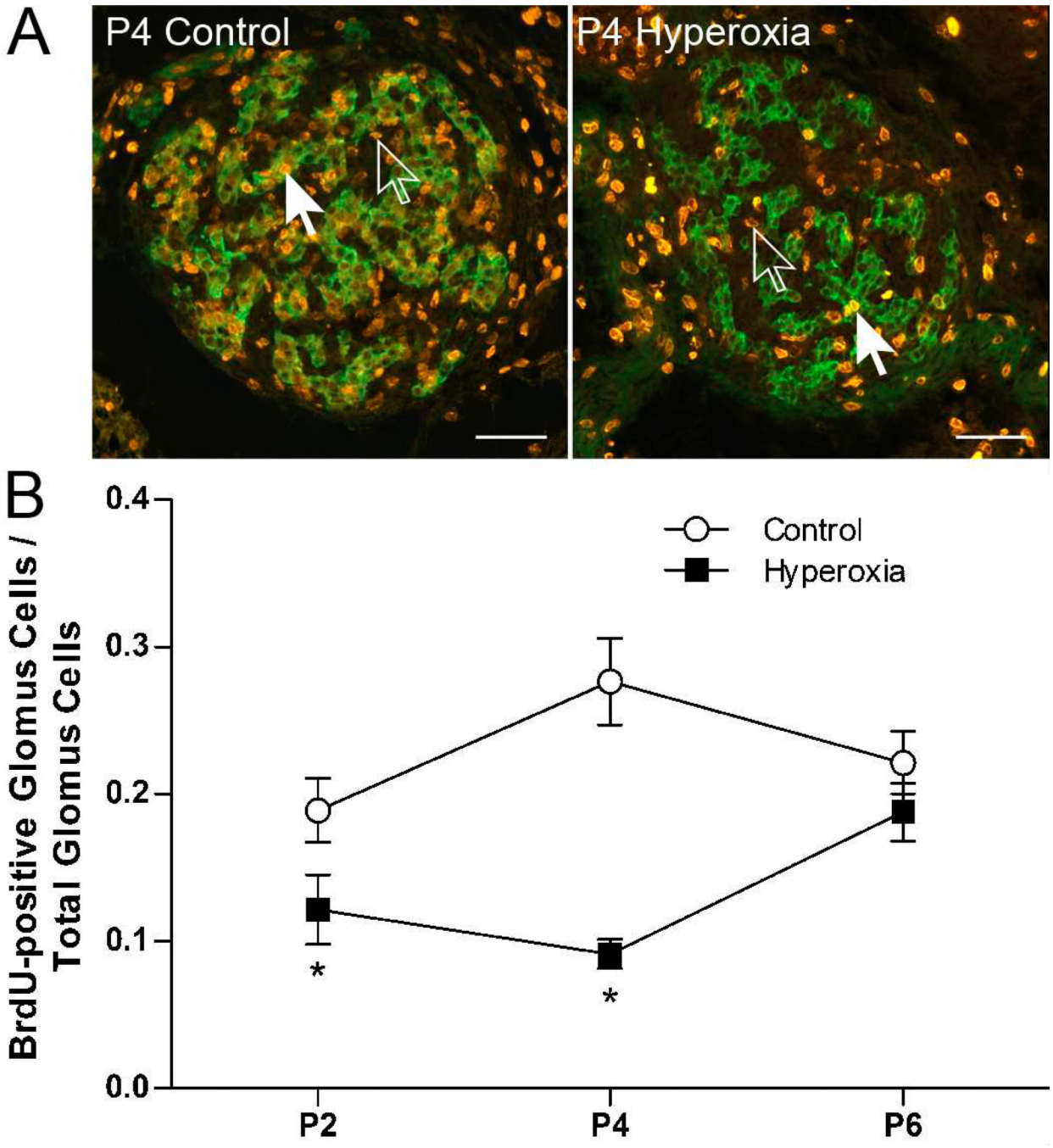

Fig. 5.

(A) Representative photomicrographs showing BrdU-positive cells in the carotid bodies of P4 rats reared in 21% O_2 (Control) or 60% O_2 (Hyperoxia). Green fluorescence indicates staining for tyrosine hydroxylase, a marker for glomus cells, and orange fluorescence indicates staining for BrdU in the nucleus of cells. Closed arrows point to BrdU-positive glomus cells (green and orange); open arrows point to BrdU-positive non-glomus cells (orange only). Scale bar = 50 μm. (B) The ratio of BrdU-positive glomus cells to the total number of glomus cells in Control and Hyperoxia rats at P2, P4, and P6. BrdU was administered 24 h prior to tissue collection, so labeled cells underwent cell division P1-P2,

P3-P4, or P5-P6, respectively. Values are mean ± SEM; n = 6 per treatment group per age. *P<0.05 vs. Control at the same age.

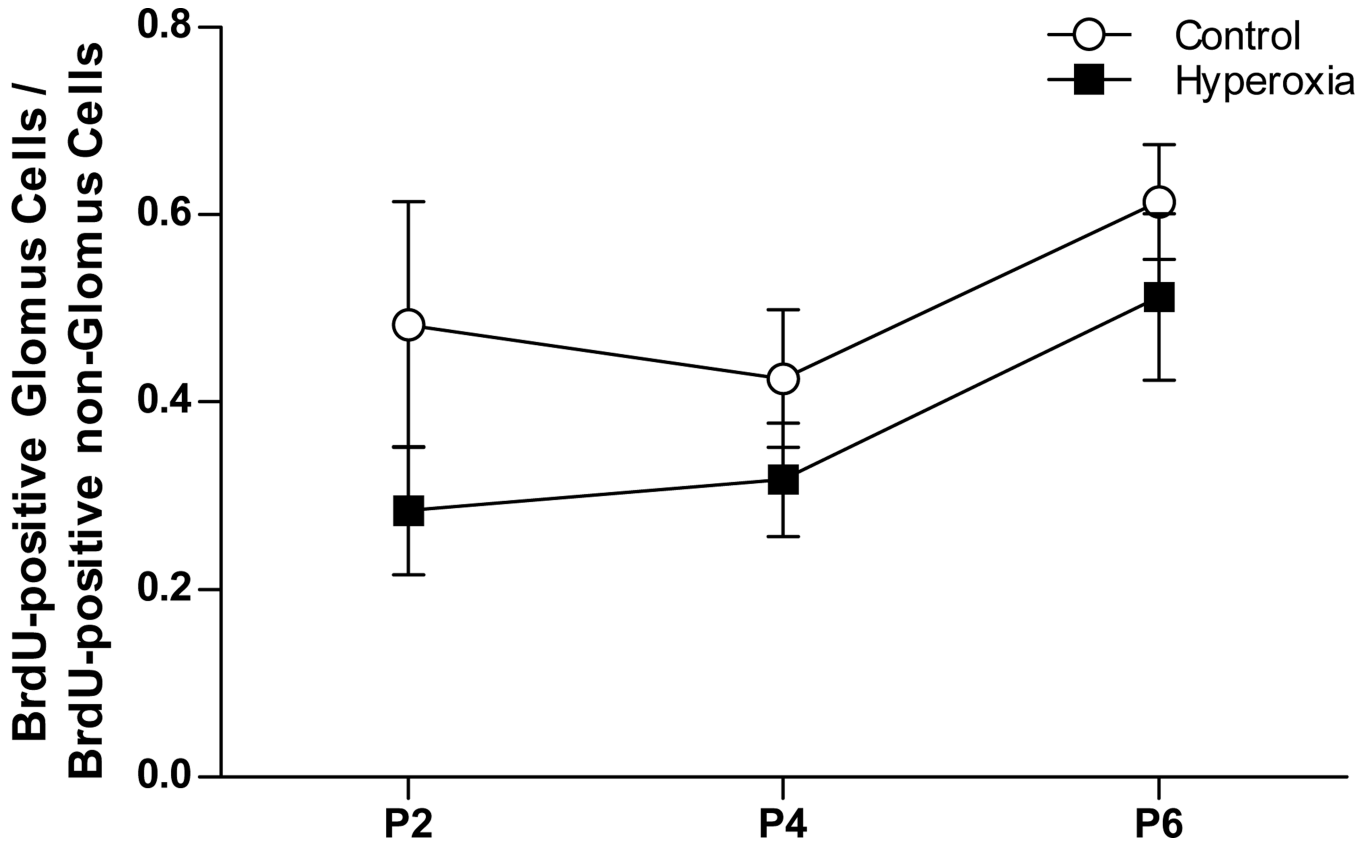

Fig. 6.

The ratio of BrdU-positive glomus cells to BrdU-positive non-glomus cells in the carotid bodies of neonatal rats reared in 21% O_2 (Control) or 60% O_2 (Hyperoxia). Carotid bodies were sampled at P2, P4, and P6, 24 h after administering BrdU. Values are mean ± SEM; n = 6 per treatment group per age. No significant differences were detected between groups.

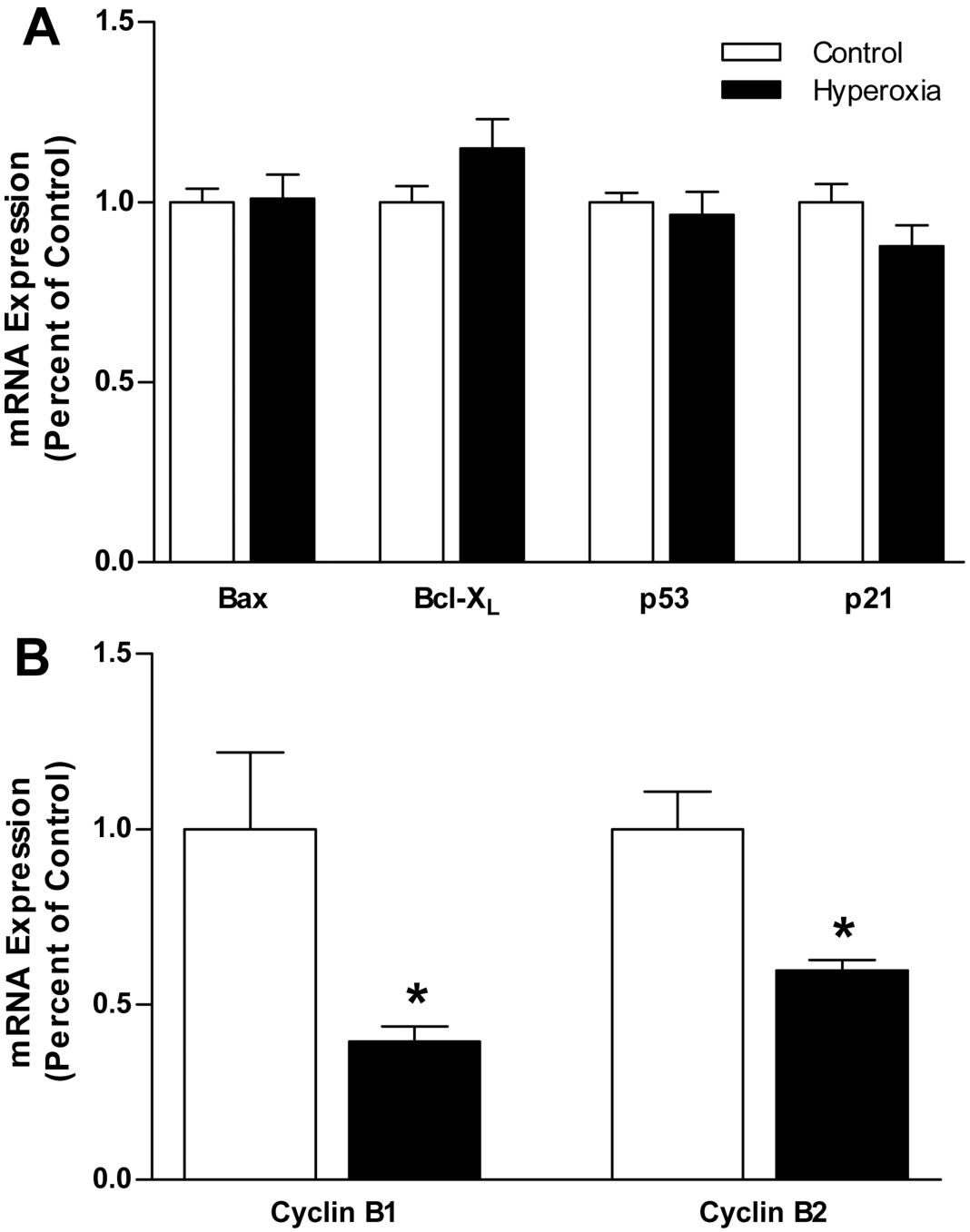

Fig. 7.

Quantitative RT-PCR analysis of (A) p21, p53, Bax, and Bcl-X_L mRNA expression and (B) cyclin B1 and cyclin B2 mRNA expression in the carotid bodies of P3 rats reared in 21% O_2 (Control) or 60% O_2 (Hyperoxia); mRNA expression was normalized to β-actin. Values are mean ± SEM; n = 7 per treatment group in panel A and 6 per treatment group in panel B. * P<0.05 vs. Control.

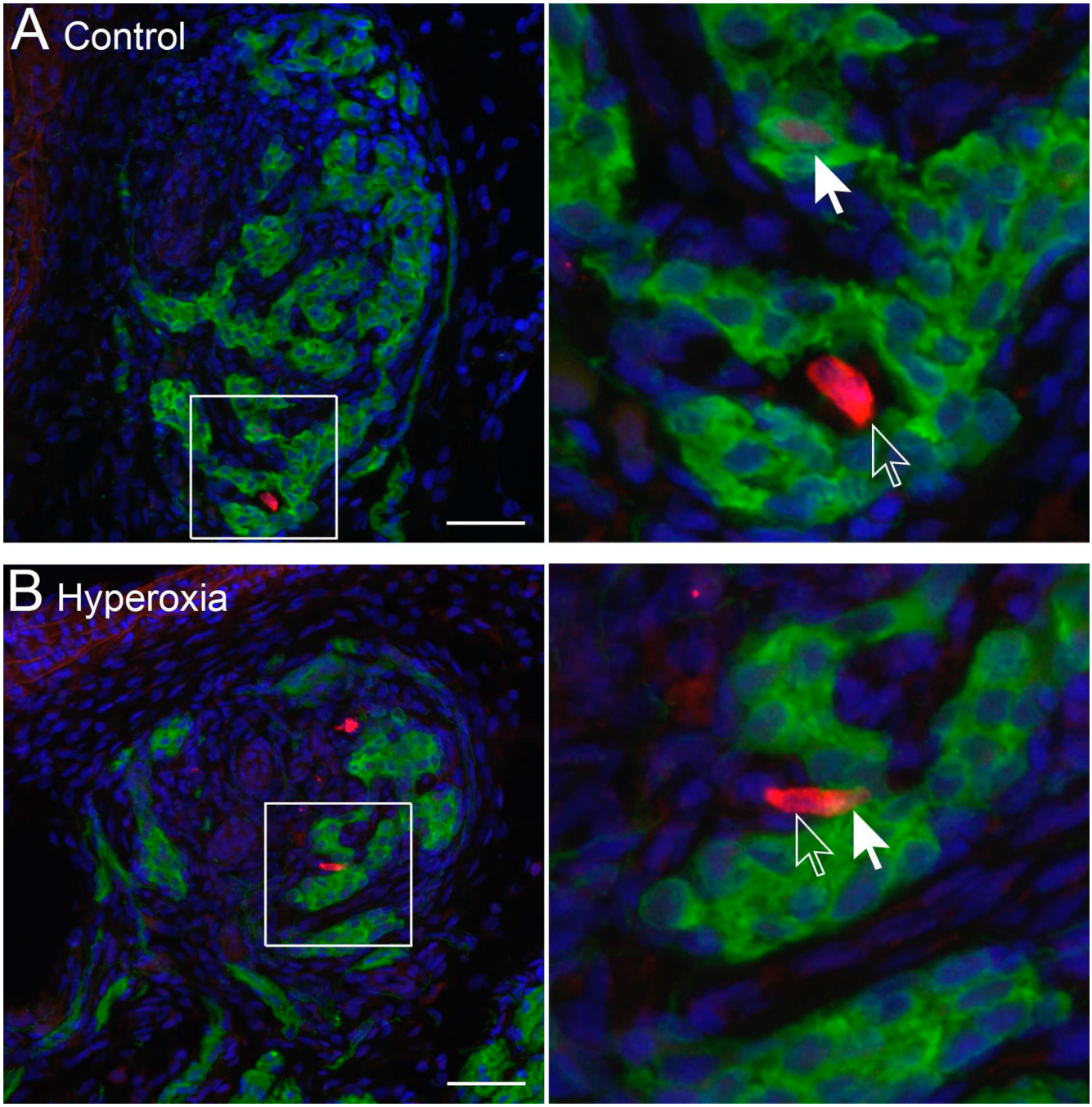

Fig. 8.

Representative photomicrographs showing p21 protein expression in the carotid bodies of P3 rats reared in (A) 21% O_2 (Control) or (B) 60% O_2 (Hyperoxia). Green fluorescence indicates staining for tyrosine hydroxylase, a marker for glomus cells, red fluorescence indicates p21, and blue fluorescence indicates nuclei (DAPI). The area indicated by the box in left panels has been enlarged (right panels) to illustrate p21-positive glomus cells (red and green; closed arrow) and p21-positive non-glomus cells (red only; open arrow). Scale bars = 50 μm.

Table 1

Primers for quantitative RT-PCR

Target Gene	Forward Primer (5'-3')	Conc. (nM)	Reverse Primer (5'-3')	Conc. (nM)	Expected Length (bp)	Annealing Temp (°C)
β-actin †	CTAAGGCCAACCGTGAAAAGAT	600	CCAGAGGCATACAGGGACAAC	100	103	65
p21	CGAGACACTCAGAGCCACA	300	GCGAAGTCAAAGTTCCACC	300	182	65
p53	ACCTCCACACCTCCACCT	300	AGATACTCAGCATACGATTTC	600	176	60
Bax	AGAGGATGATTGCTGATGTG	100	CGGAGGAAGTCCAGTGTC	600	205	60
Bcl-X_L	GGACTGAAGCCCCAGAAGA	600	CAAACTCATCGCCAGCCTC	600	192	60

† used as reference gene

Respir Physiol Neurobiol. Author manuscript; available in PMC 2013 March 15.